

DNAMOTIFTOKENIZER: TOWARDS BIOLOGICALLY INFORMED TOKENIZATION OF GENOMIC SEQUENCES

Xiaoxiao Zhou¹, Zihan Wang², Jingbo Shang², Yang E. Li^{1*}

¹Washington University in St. Louis, ²University of California San Diego

xiaoxiao.zhou@wustl.edu, ziw224@ucsd.edu

jshang@ucsd.edu, yeli@wustl.edu

ABSTRACT

DNA language models have advanced genomics, but their downstream performance varies widely due to differences in tokenization, pretraining data, and architecture. We argue that a major bottleneck lies in tokenizing sparse and unevenly distributed DNA sequence motifs, which are critical for accurate and interpretable models. To investigate, we systematically benchmark k-mer and Byte-Pair Encoding (BPE) tokenizers under controlled pretraining budget, evaluating across multiple downstream tasks from five datasets. We find that tokenizer choice induces task-specific trade-offs, and that vocabulary size and tokenizer training data strongly influence the biological knowledge captured. Notably, BPE tokenizers achieve strong performance when trained on smaller but biologically significant data. Building on these insights, we introduce DNAMotifTokenizer, which directly incorporates domain knowledge of DNA sequence motifs into the tokenization process. DNAMotifTokenizer consistently outperforms BPE across diverse benchmarks, demonstrating that knowledge-infused tokenization is crucial for learning powerful, interpretable, and generalizable genomic representations.

1 INTRODUCTION

Recent advances in artificial intelligence (AI) and large language models (LLMs) have transformed nearly every field of biological research. By analyzing complex, noisy, and large-scale datasets, these models can uncover hidden patterns, generate predictions, and accelerate the discovery of new biological knowledge and molecular structures (Nature Methods, 2024). In genetics, building on the remarkable success of text-based LLMs, researchers have developed DNA language models (DNA-LMs) to capture the latent “grammar” of genomic sequences. These models are being leveraged to improve DNA sequence design, investigate the genetic basis of evolution, and interpret genetic mutations underlying human traits and diseases.

Over the past few years, a series of DNA-LMs has emerged (see Figure 1a). Early efforts, such as DNABERT-1 (Ji et al., 2021), introduced k-mer-based tokenizers and transformer architectures to model DNA sequences, laying the foundation for various downstream applications. DNABERT-2 (Zhou et al., 2023) extended this idea by introducing byte-pair encoding (BPE)-based (Sennrich et al., 2015) tokenizer and pretrained on multi-species genomes. A large-scale model, Nucleotide Transformer (Dalla-Torre et al., 2025), has scaled up in both parameter size and training corpus, improving accuracy and generalizability. The HyenaDNA (Nguyen et al., 2023) has explored long-context modeling to better capture distal dependencies in the genome. More recently, Evo-2 (Brixi et al., 2025) has been developed to expand prediction and design across DNA, RNA, and proteins. Collectively, these models underscore both the promise and challenges of scaling DNA-LMs for biological discovery, including regulatory element prediction, non-coding genetic variant interpretation, and DNA sequence designs.

Despite their superb fine-tuning performance in downstream tasks, current DNA-LMs often exhibit poor zero-shot generalization to new tasks (Patel et al., 2024). The bottleneck lies largely in the DNA tokenization process, which breaks down raw DNA sequences into fundamental units for the

*Corresponding author

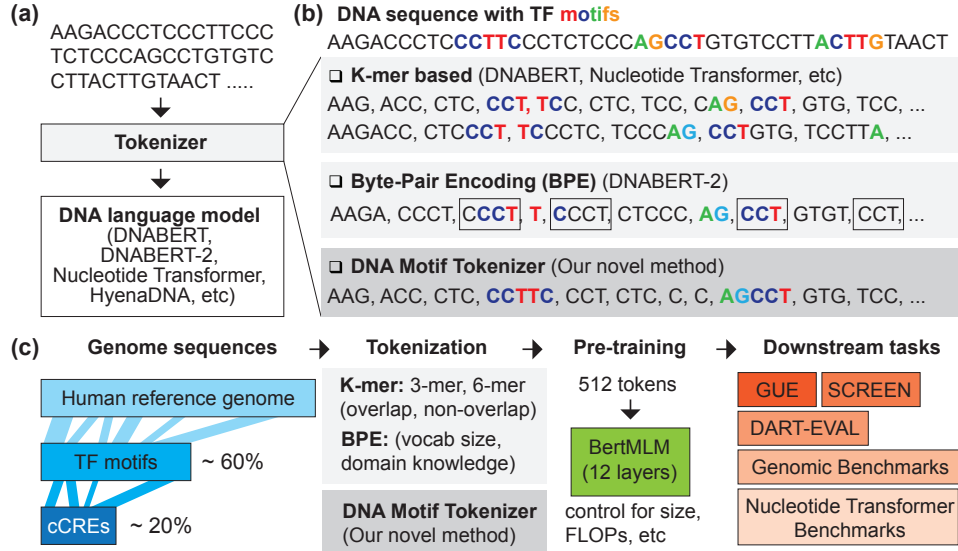


Figure 1: Overview Strategy and Pipeline. **(a)** DNA language-modeling pipeline. **(b)** State-of-the-art genomic tokenizers and DNA Motif Tokenizer. **(c)** Domain knowledge for tokenizer construction, our novel DNAMotifTokenizer, pretraining and downstream evaluation workflow.

model to process (see Figure 1b). Standard tokenization strategies, such as fixed k-mers or subword methods like byte-pair encoding (BPE), often fail to efficiently capture these biologically meaningful DNA motifs. It is critical to optimize the DNA tokenization step towards the development of accurate, interpretable, and generalizable models.

In this work, we systematically investigate the impact of tokenization on DNA-LMs with different categories of human genomic sequences (see Figure 1c). Under controlled pretraining settings, we benchmark a variety of k-mer and BPE-based tokenizers across five distinct datasets spanning multiple downstream tasks. Our analysis reveals that the choice of tokenizer induces significant task-specific trade-offs, and we find that incorporating domain knowledge, DNA sequence motifs, is essential for learning more robust DNA representations.

To address this, we introduce DNAMotifTokenizer, a novel strategy that directly incorporates domain knowledge of DNA sequence motifs into the DNA tokenization process. In our comprehensive benchmarks, DNAMotifTokenizer consistently outperforms BPE-based tokenizers across diverse tasks, demonstrating that knowledge-infused tokenization is crucial for learning powerful, interpretable, and generalizable genomic representations.

Our main contributions can therefore be summarized as follows: (1) We introduce Search Candidate cis-Regulatory Elements by ENCODE (SCREEN) benchmarking dataset, which contains a standardized, comprehensive, and well-annotated human functional genomic regulatory elements. (2) We provide the first systematic evaluation of DNA tokenization strategies under controlled pretraining, revealing task-specific trade-offs. (3) We propose DNAMotifTokenizer, a motif-aware tokenizer that directly encodes biologically meaningful sequence motifs. DNAMotifTokenizer consistently outperforms or achieves the state-of-the-art performance, highlighting the necessity of introducing domain knowledge for genomic representation learning. The code, data, and pre-trained model are available in **supplementary materials**.

2 BACKGROUND

In natural language processing (NLP), tokenization is a critical step that converts text into a format suitable for computational models. Similarly, genomic sequences can be viewed as a “language” encoding complex information that regulates gene expression in organs, tissues, and cell types across healthy and disease conditions.

Table 1: Comparison of state-of-the-art DNA-LMs

Model	Model Size	Tokenizer	Pretrain Data
HyenaDNA	<6.6M	1mer	Human reference genome
DNAbert1-3mer	86M	3mer, stride=1	Human reference genome
DNAbert1-6mer	89M	6mer, stride=1	Human reference genome
DNAbert2	117M	BPE, vocab size=4096	135 species genomes
NT-HumanRef	500M	6mer, stride=6	Human reference genome
NT-1000GG	500M/2.5B	6mer, stride=6	3202 human genomes
NT-HumanRef	2.5B	6mer, stride=6	850 species genomes
MxDNA	100M	Customized	Human reference genome

The k-mer and BPE-based tokenizers are commonly used in state-of-the-art DNA-LMs(Table 1). HyenaDNA (Nguyen et al., 2023) uses a 1-mer tokenizer and a decoder-only architecture with the Hyena operator to model long-range dependencies. DNABERT-1 (Ji et al., 2021) tokenized the genome with overlapping k-mers and trained separate models for each, substantially outperforming several downstream tasks. Nucleotide Transformer (Dalla-Torre et al., 2025) employs non-overlapping 6-mer tokenization and leverages large-scale pretraining across thousands of human individual genomes, and hundreds of species. Zhou et al. (2023) proposed DNABERT-2, which uses a byte-pair encoding (BPE) tokenizer inspired by NLP. MxDNA (Qiao et al., 2024) introduced a learnable tokenizer using a Mixture-of-Experts framework (Shazeer et al., 2017) and deformable convolutions (Dai et al., 2017).

Despite these advances, the field lacks a systematic comparison of how tokenizer choice alone affects model performance. Existing models differ not only in tokenizers but also in architecture, model size, and pretraining data, which confound direct comparisons (Table 1). This limits our ability to reason about what makes a tokenizer effective and to design better ones.

In addition, DNA is composed of highly repetitive, short, sparse, unevenly distributed, but conserved DNA sequence motifs across 600 million years of bilaterian evolution Nitta et al. (2015), largely represented by transcription factor (TF) binding motifs. The complexity of gene regulation often arises from the specific rearrangement and combination of these conserved motifs into context-specific regulatory elements Wong et al. (2020). Standard tokenization methods, which are agnostic to biological function, often arbitrarily split these meaningful motifs into smaller, non-functional tokens (see Figure 1b). As a result, it hampers DNA-LMs’ ability to learn biologically meaningful representations of genomic sequences and complicates downstream model interpretation.

To address these issues, we developed a controlled benchmarking framework to systematically assess the tokenizer’s influence and identify key factors for effective design. Guided by our findings, we propose DNAMotifTokenizer, a novel tokenizer that takes a significant step towards a more biologically informed tokenization of genomic sequences. By embedding the essential “grammar” of gene regulation into its vocabulary, DNAMotifTokenizer enables DNA-LMs to better capture the complex relationships between sequence and function. We also assess the generalizability, stability, complexity, and interpretability of our approach.

3 DATA

3.1 GENOMIC SEQUENCES

Human reference genome: We use the most widely used human reference genome, version hg38 (GRCh38) (Consortium, 2013), which incorporates improved accuracy and coverage over previous releases.

Annotation of motif regions: We download the genome-wide JASPAR CORE TF motif predictions on the human reference genome (hg38) from the UCSC Genome Browser (Lee et al., 2020)(Raney et al., 2014). For BPE training, we extract all predicted motif sequences and merge any overlapping ones to create a non-redundant set. The resulting set of motif sequences covers approximately 59.84% (See Table C.1) of the human genome.

Annotation of cCREs: Candidate cis-regulatory elements (cCREs) are functional regulatory units in the genome, such as promoters and enhancers, that are typically hundreds of base pairs long. These regions often contain multiple TF motifs and are crucial for controlling when and where genes are expressed. For this study, we download human cCRE annotations from The Encyclopedia of DNA Elements(ENCODE), which provide genomic coordinates and regulatory classifications (Moore et al., 2020)(Luo et al., 2020). We extract the corresponding DNA sequences for BPE training, which constitute approximately 20.32% (See Table C.2) of the human reference genome.

3.2 BENCHMARK DATASETS

Genome Understanding Evaluation(GUE): Genome Understanding Evaluation (GUE) dataset was collected by (Zhou et al., 2023), consisting of 28 distinct datasets across 7 tasks and 4 species, with DNA inputs ranging from 70 to 1000 base pairs (bp). The metric we use is the Matthews Correlation Coefficient (MCC) (see **Appendix**).

Nucleotide Transformer Benchmarks: Nucleotide Transformer (NT) benchmarks were collected by (Dalla-Torre et al., 2025), it includes 18 datasets across 4 tasks only on humans. For this dataset, MCC is employed as the metric.

Dart-Eval: This dataset was introduced by (Patel et al., 2024) and contains five tasks. In our experiments, we focus on tasks 1–3. Accuracy (ACC) served as the evaluation metric. Task 1 involves distinguishing cCRE regions from background sequences. Task 2 requires identifying transcription factor (TF) binding motifs within background sequences. Task 3 entails classifying sequences specific to five different cell types against background sequences.

Genomic Benchmarks: This dataset was collected by (Grešová et al., 2023), it includes 9 tasks, across 9 species. We only use human related datasets. MCC is used as the metric.

SCREEN: We create this benchmark dataset by first downloading the cCREs on hg38 from the SCREEN interface (Moore et al., 2020), a platform for searching and visualizing the ENCODE Registry of candidate cis-Regulatory Elements (cCREs). This Registry contains 2,348,854 human cCREs, classified into eight categories, including promoter-like signatures (PLS), proximal and distal enhancer-like signatures (pELS, dELS), and CTCF- or TF-associated accessible elements (CA, CA-CTCF, CA-H3K4me3, CA-TF, TF). We generated a negative superset by taking the complement of all cCRE regions and dividing it into 300 base pair (bp) segments. For each cCRE category, we then randomly sample from this superset to obtain the same number of sequences as in the corresponding negative set. This procedure yielded eight datasets, each containing an equal number of positive and negative sequences.

4 METHOD

4.1 TOKENIZERS

K-mer tokenizer: A k-mer is a substring of length k from a DNA or RNA sequence (Moeckel et al., 2024). K-mers can be generated in two ways: overlapping, by sliding a window one base at a time to capture all subsequences, or non-overlapping, by moving the window in steps of k to produce disjoint subsequences. In our experiments, we test overlapping 3-mer and 6-mer implemented by DNABERT-1 (Ji et al., 2021), and non-overlapping 6-mer implemented by Nucleotide Transformer (Dalla-Torre et al., 2025), respectively.

BPE tokenizer: BPE is a learnable subword tokenization algorithm that iteratively merges the most frequent pairs of characters or subwords in a training corpus to build a vocabulary of common subwords (Sennrich et al., 2015). The resulting merge rules, based on pair frequency, are recorded and applied to tokenize new sequences consistently, allowing the model to capture recurring patterns efficiently. The BPE tokenizer for DNA sequences was introduced by DNABERT-2. We use the BPE tokenizer pretrained by DNABERT-2 and also train our own BPEs on human reference genome, motif enriched genomic regions, and cis-regulatory element (cCRE) regions (see **Section 3**). Three vocabulary sizes were explored: 4096 (matching DNABERT-2), 2048, and 1024. Each BPE was initialized with the DNA alphabet (A, T, C, G, N) and five special tokens ([PAD], [UNK], [CLS], [SEP], [MASK]), with a minimum frequency threshold of 100.

Others: MxDNA (Qiao et al., 2024) is excluded from comparison due to a lack of publicly available pre-trained weights.

DNA Motif Tokenizer: We develop DNAMotifTokenizer, a novel tokenizer designed to understand the language of the genome by directly embedding biological domain knowledge—specifically, TF motifs, the functional ‘words’ of the genome—into its vocabulary. In addition, we design a greedy algorithm to tokenize the incoming sequences with our customized vocabulary. See **Section 7** for more details.

4.2 MODELS

Architecture: We adopt a BERT-based masked language model architecture (BertMLM) (Devlin et al., 2019) for our experiments. The model uses the Transformer encoder architecture (Vaswani et al., 2017) with 12 layers and 12 attention heads and a hidden size of 768, resulting in intermediate feed-forward layers of size 3072. The maximum input sequence length is 512 tokens, and the model uses learnable positional embeddings up to this length. Dropout Srivastava et al. (2014) is applied to both the attention probabilities and hidden layers with a rate of 0.1, and the GELU (Hendrycks & Gimpel, 2016) activation function is used throughout. The model vocabulary size is changed according to the tokenizer used, and a type vocabulary of size 2 is included to distinguish segment embeddings. All parameters are initialized with a standard deviation of 0.02.

Pre-training: During pre-training, we strictly control all experiments to ensure comparability by keeping the models’ floating-point operations per second (FLOPs) consistent. All tokenizers are applied to the human reference genome (chromosomes 1–22, X, Y, and M), and the tokenized sequences are sequentially split into segments of 512 tokens to serve as input for the BertMLMs. Segments containing more than 50% N tokens are discarded. Each model is trained with a batch size of 96 for 200,000 steps, using a learning rate of 4e-5, Adam optimizer parameters ($\beta_1 = 0.9, \beta_2 = 0.98, \delta = 1 \times 10^{-6}$), weight decay of 0.01, a masked language modeling probability of 0.15, and 10,000 warmup steps.

Evaluation: During model evaluation, we fine-tune the pre-trained models on five benchmark datasets (see Section 3 for details). Most fine-tuning hyperparameters are consistent across models, varying primarily in the maximum input length, which is adjusted per tokenizer. Performances are measured using the Matthews Correlation Coefficient (MCC) for four datasets, and Accuracy (ACC) for the DART-Eval benchmarking dataset.

We compare the vocabulary similarities by calculating the pairwise Jaccard Index. We also generate Venn diagrams illustrating their word overlap (Hulsen, 2021). See **Appendix** for more details.

5 BENCHMARKING OF STATE-OF-THE-ART TOKENIZERS

A variety of k-mer and BPE-based tokenizers are used in state-of-the-art DNA-LMs. However, these models vary in architecture, model size, and pre-training data (see Table 1), making it difficult to isolate the impact of the tokenizer on model performance. To systematically evaluate various DNA tokenizers, we design experiments on the human reference genome with strictly controlled pre-training and fine-tuning protocols (see **Section 4.2**). These DNA tokenizers include 3-mer (overlap), 6-mer (overlap) from DNABERT-1, 6-mer (non-overlap) from Nucleotide Transformer, the original BPE from DNABERT-2, and a custom BPE tokenizer (vocabulary size = 4096) trained on the human reference genome (see Figure 2a). We fine-tune each pre-trained model on five distinct benchmarking datasets and compare the average performance of each DNA tokenizer (Figure 2b). Our findings reveal a clear performance trade-off: although k-mer-based tokenizers achieve higher performance on specific tasks, like splicing site prediction, no single tokenizer consistently outperformed the others. Overall, BPE tokenizers achieve more robust performance, surpassing k-mer tokenizers in four of the five benchmark datasets. More detailed results for each task across all benchmark datasets are provided in the **Appendix**.

We use the NT-benchmarks to investigate the zero-shot ability, where k-mer tokenizers consistently outperformed BPE tokenizers. Both overlapping and non-overlapping k-mer tokenizers struggled to cluster four distinct genomic elements, while BPE tokenizers performed better at separating enhancers and promoters from other DNA sequences (Figure 2c). Furthermore, we leverage the most

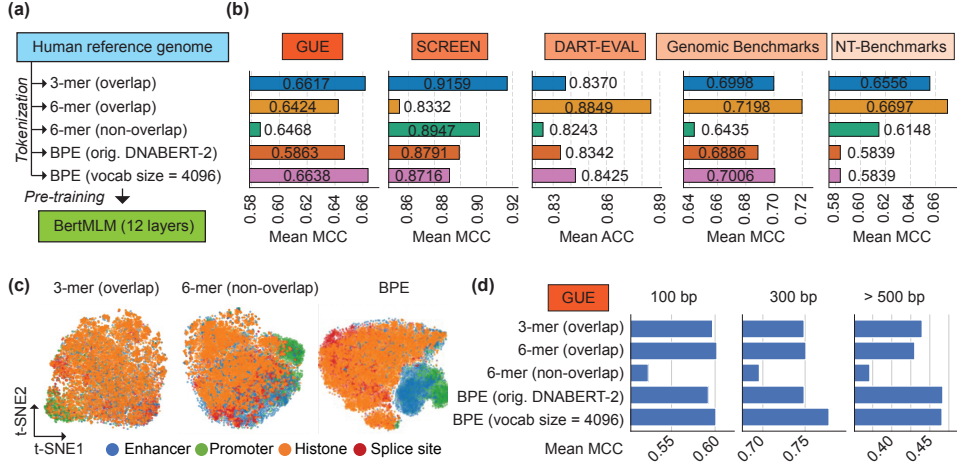


Figure 2: Benchmarking of state-of-the-art Tokenizers. **(a)** Overview benchmarking pipeline for overlap k-mer, non-overlap k-mer, and BPE-based tokenizers trained by DNABERT-2 and trained on human genome (vocabulary size 4,096). **(b)** Evaluation on five benchmarking datasets. **(c)** Zero-shot performance of k-mer and BPE-based tokenizer on genomic region classification. **(d)** BPE-based tokenizer outperforms in longer DNA sequence from GUE dataset.

comprehensive GUE benchmark and group downstream tasks by the length of DNA sequences. We find that k-mer tokenizers performed marginally better on shorter sequences (100 bp), whereas BPE tokenizers excel on longer ones (>500 bp) (Figure 2d), which is consistent with previous work (Zhou et al., 2023). Taken together, we conclude that BPE-based tokenizers achieve more robust performance on both zero-shot and fine-tuning tasks and are more generalizable for predictions involving longer DNA sequences.

6 WHAT MAKES A GOOD BPE TOKENIZER?

To better optimize BPE tokenizers for genomic sequences, we examine two key dimensions: vocabulary size, which determines token granularity and model performance, and domain knowledge, which grounds tokens in biologically meaningful units.

6.1 SIZE MATTERS: VOCABULARY SCALING

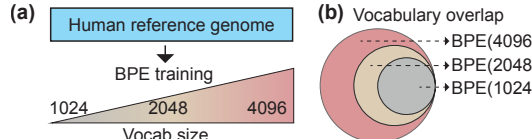


Figure 3: BPE with Different Vocabulary Size. **(a)** Training BPEs with vocabularies of 1,024, 2,048, and 4,096 tokens. **(b)** Vocabulary overlap across the trained BPEs.

Using the human reference genome, we first train BPE tokenizers with three vocabulary sizes: 1,024, 2,048, and 4,096 (Figure 3a). We overlap token vocabularies and find that they were nested (Figure 3b). For example, each larger set (e.g. BPE 2048) contains all tokens from the smaller ones (e.g., BPE 1024). This hierarchical structure means longer vocabularies are built by merging shorter, existing tokens, leading to a marginal increase in average token length (Figure B.1a) and a wider distribution of token frequencies (Figure B.1 b). Next, to quantify the information gained by expanding the vocabulary, we compute the Shannon entropy for the set of novel tokens introduced at each increase in vocabulary size. For instance, BPE (2048-1024) refers to the new tokens learned by the BPE 2048-token vocabulary that were not present in the BPE 1024-token vocabulary, with the same logic applying to BPE (4096-2048). We observe a significant increase (Wilcoxon test) in mean entropy (red triangle) across BPE (1024), BPE (2048-1024) and BPE (4096-2048), suggesting that larger vocabularies capture more complex and diverse tokens within the genomic sequences (Figure B.1c). Last, we fine-tune models using each of these BPE tokenizers on five benchmark datasets

to evaluate their downstream performance (Table 2). Counterintuitively, the more diverse and longer tokens captured by a larger vocabulary did not translate to better predictive performance. In fact, our findings consistently show that a more concise token vocabulary led to superior overall results.

In summary, we suggest that increasing the BPE vocabulary size beyond a certain point introduces information redundancy, which may negatively impact model performance.

Table 2: Performance of BPE models with varying vocabulary sizes across five benchmark datasets

Model	GUE Ave. MCC	SCREEN Ave. MCC	DART-EVAL Ave. ACC	Genomic Benchmarks Ave. MCC	NT-Benchmarks Ave. MCC
BPE(DNABERT2)	0.6468 \pm 0.1242	0.8791 \pm 0.0224	0.8342 \pm 0.0328	0.6886 \pm 0.1721	0.5839 \pm 0.1016
BPE(4096)	0.6638 \pm 0.122	0.8717 \pm 0.0294	0.8425 \pm 0.0408	0.7006 \pm 0.1565	0.5839 \pm 0.0945
BPE(2048)	0.6684 \pm 0.1302	0.8743 \pm 0.033	0.8451 \pm 0.0531	0.7021 \pm 0.1584	0.595 \pm 0.1052
BPE(1024)	0.673 \pm 0.127	0.8781 \pm 0.0269	0.8604 \pm 0.0471	0.7069 \pm 0.1556	0.5988 \pm 0.1121

6.2 INFORMATIVE TOKENS: ADDING DOMAIN KNOWLEDGE

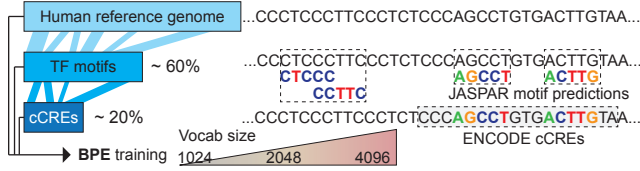


Figure 4: Training BPE on Domain Knowledge. **Left:** Train BPE tokenizers on the whole human genome, TF motif regions (60% of the genome), and cCRE regions (20% of the genome) with different vocabulary size. **Right:** Illustration of TF motifs and cCREs distributions on the genome.

We hypothesize that training BPE tokenizers on biologically meaningful subsets of the genome, rather than the entire genome, could yield more effective models. To test our hypothesis, we train BPE tokenizers with various vocabulary sizes on three distinct datasets, including the full human reference genome, genomic regions predicted as TF motifs, and biological function-enriched cCREs regions, to assess whether data selection improves tokenization (see Section 3 and Figure 4). We first compare the BPE token vocabularies learned from the human reference genome, motif, and cCRE regions by calculating their pairwise Jaccard Similarity Index (Figure B.2a). Our analysis reveals that the BPE tokenizer trained on motif regions produced the most distinct vocabulary, compared to those trained on the whole genome or cCREs. For example, with a vocabulary size of 1024, the motif-trained BPE learned 415 unique tokens (40.5%) not found in the other two vocabularies (Figure B.2b). Although we find no significant differences in token length distribution (Figure B.2c), the motif BPE generated a higher proportion of low-frequency tokens when applied to the human reference genome (Figure B.2d). We also observe the same pattern for BPE tokenizers with larger vocabulary sizes. Next, we rigorously evaluate and compare the downstream performance of models trained with each tokenizer (Table 3). Our results show that models with BPE tokenizers trained on motif and cCRE regions can achieve comparable performance to those trained on the whole human genome, regardless of vocabulary size.

These results, consistent across five benchmark datasets, suggest that BPE tokenizers can be trained more efficiently using curated datasets enriched with domain knowledge, without sacrificing model performance.

7 OUR NOVEL DNAMOTIFTOKENIZER

Building on aforementioned insights, we would like to ask whether domain knowledge can be directly integrated into the tokenizer’s design to improve performance. To test it, we develop DNAMotifTokenizer, a novel tokenizer that directly incorporates TF motifs into the vocabulary and applies a greedy search algorithm to tokenize the corresponding patterns in DNA sequences (Figure 5).

Table 3: Performance of BPE models with varying vocabulary size and domain knowledge

Vocab Size	Domain Knowledge	GUE	SCREEN	DART-EVAL	Genomic Benchmarks	NT-Benchmarks
		Ave. MCC	Ave. MCC	Ave. ACC	Ave. MCC	Ave. MCC
4096	hg38	0.6638 ± 0.122	0.8717 ± 0.0294	0.8425 ± 0.0408	0.7006 ± 0.1565	0.5839 ± 0.0945
	cCREs	0.6552 ± 0.1268	0.8719 ± 0.0333	0.8425 ± 0.0451	0.699 ± 0.1642	0.5723 ± 0.0896
	motifs	0.6522 ± 0.1299	0.8694 ± 0.0338	0.8309 ± 0.0331	0.6844 ± 0.1644	0.5764 ± 0.0997
2048	hg38	0.6684 ± 0.1302	0.8743 ± 0.033	0.8451 ± 0.0531	0.7021 ± 0.1584	0.595 ± 0.1052
	cCREs	0.6645 ± 0.1283	0.8767 ± 0.0279	0.8382 ± 0.0416	0.6993 ± 0.1685	0.5973 ± 0.1108
	motifs	0.6695 ± 0.1273	0.8769 ± 0.0231	0.8392 ± 0.0499	0.6868 ± 0.1617	0.5902 ± 0.1057
1024	hg38	0.673 ± 0.127	0.8781 ± 0.0269	0.8604 ± 0.0471	0.7069 ± 0.1556	0.5988 ± 0.1121
	cCREs	0.6743 ± 0.1244	0.8793 ± 0.0242	0.8458 ± 0.0556	0.7039 ± 0.1633	0.5954 ± 0.1097
	motifs	0.6684 ± 0.1278	0.8777 ± 0.0244	0.8494 ± 0.0478	0.7005 ± 0.163	0.5954 ± 0.1143

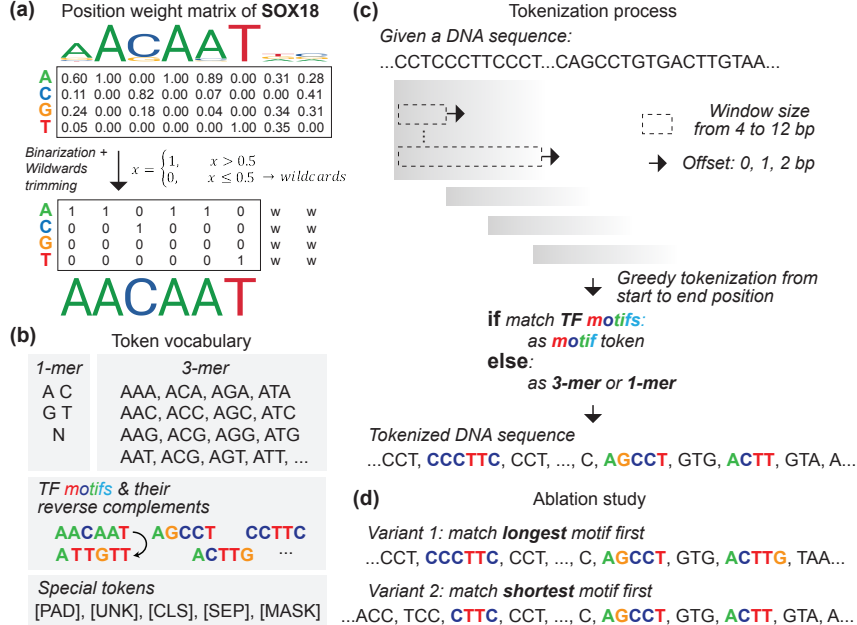


Figure 5: Overview of DNAMotifTokenizer. **(a)** Pre-processing of motif’s probability weight matrix. **(b)** The constructed vocabulary, consisting of special tokens, motif tokens, 3-mer tokens, and 1-mer tokens. **(c)** The greedy tokenization algorithm, which by default randomly selects among matched motifs at each position. **(d)** Two deterministic variants of the tokenizer: matching by the longest motif first or by the shortest motif first.

7.1 ALGORITHM

Motif processing: Motifs are short, recurring patterns in DNA, RNA, or protein sequences that are frequently associated with specific biological functions. In this work, we focus on TF motifs, which are short DNA sequences that are bound by transcription factor proteins to regulate gene expression. The TF motifs are generally represented in the form of position weight matrices (PWM)(Stormo, 2000), which indicate the probability of each nucleotide occurring at each position within the motif. We download motif PWMs from the JASPAR 2024 motif library (Sandelin et al., 2004)(Rauluseviciute et al., 2024), which is a widely used, open-access repository. We use the vertebrate library, which contains 879 non-redundant motifs. As most TF motifs range in length from 5 to 12 base pairs (bp), we exclude any motifs longer than 12 bp from our analysis. To incorporate TF motifs into our vocabulary, we binarize their PWMs and encode them into fixed sequences (Figure 5a). For each TF PWM, we apply a threshold probability of 0.5. Positions with lower probability are defined as wildcard positions. Subsequently, we discard wildcard positions at both ends of the motif. For the remaining positions, we encode them using the nucleotide with the highest probability.

Our customized token vocabulary: In addition to the motif sequences defined in the previous section, we include their reverse complements in the vocabulary. Furthermore, we add 3-mer, 1-mer(A, T, C, G, N), and five special tokens, namely [PAD], [UNK], [CLS], [SEP], and [MASK],

to form our final vocabulary. Our final vocabulary has 901 tokens in total, including 827 motif sequences, 64 3-mer, 5 1-mer(A, T, C, G, N), and 5 special tokens (Figure 5b).

Tokenization algorithm: With our customized vocabulary established, we implement a greedy, non-overlapping tokenization algorithm. The algorithm scans an incoming DNA sequence from left to right, using a sliding window that varies from 4 to 12 bp in length. We recognize that a single base-pair shift can cascade and alter the entire tokenized output. To mitigate this sensitivity without a significant loss in computational efficiency, we incorporate local flexibility by allowing for a 0 to 2 bp offset to the right. At each position, if the subsequence within the window matches one or more motifs in our vocabulary, one is selected at random to serve as the token. If no motif match is found, the sequence is tokenized using fallback 3-mer or 1-mer representations (Figure 5c). The pseudocode is shown as Algorithm 1 in **Appendix**.

7.2 EVALUATION PERFORMANCE

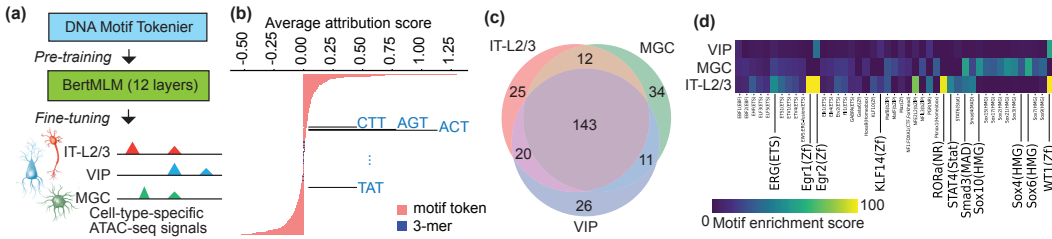


Figure 6: Interpretation of DNAMotifTokenizer. (a) Workflow for the multiclass cell-type ATAC-seq classification task. (b) Distribution of average attribution scores for k-mer and motif tokens on the test set (10%). The motif tokens exhibit the strongest influence on model predictions. (c) Overlap between top 200 highest-attribution tokens from three cell types. (d) Highly attributed motif tokens matched with motif enrichment results from Li et al. (2023).

Interpretability: We collected single-nucleus ATAC-seq (snATAC-seq) data generated from three diverse brain cell types: intratelencephalic neurons from cortical layer 2/3 (ITL23), VIP-positive GABAergic neurons (VIP), and Microglia (MGC) Li et al. (2023). We identified cell-type-specific ATAC-seq peak regions, which serve as prediction targets (Figure 6a). To control the vocabulary size and achieve fair comparison, we then fine-tuned our DNAMotifTokenizer models on this dataset. Then, we performed token attribution analysis using Integrated Gradients Sundararajan et al. (2017) on the test set (10%). For each token, we computed its attribution score toward the true class label and then averaged the scores; Tokens with attribution scores farther away from zero—either positive or negative—indicate stronger influence on the model’s prediction (Figure 6b). By ranking them, we found that in our DNAMotifTokenizer model, most of the highly influential tokens correspond to motif tokens (in red), whereas the k-mer tokens (in blue) generally had attribution scores close to zero. We selected the top 200 most contributive motif tokens for each cell type. The Venn plot indicates that DNAMotifTokenizer not only utilizes 143 motif tokens shared between three cell types, but also uses 25, 26, 34 cell-type-specific motif tokens for prediction in ITL23, VIP, MGC, respectively (Figure 6c). In addition, we compared these most contributive motif tokens with the enriched motifs for each cell type reported in the original paper Li et al. (2023). We showed top-matched motifs from three cell types as a heatmap (Figure 6d). In ITL23 cell type, motifs from the WT1, RORA, Egr, and KLF families are captured and enriched, whereas only WT1, and Egr2 are captured in the VIP cell type. In MGC cell type, SOX family motifs are captured and enriched. These results demonstrate the interpretability of motif tokens introduced by DNAMotifTokenizer in various cell types.

Downstream tasks: We evaluate the downstream performance of models trained with DNAMotifTokenizer. We reveal that DNAMotifTokenizer consistently matches or exceeds the performance of BPE models (Table 4). For DART-EVAL tasks, the synthetic sequences may not exhibit a natural motif distribution, which can affect the classification performance of our method.

Generalizability: We finetuned our models on Yeast and Mouse datasets from the GUE dataset. Compared to published k-mer and BPE tokenizers learnt from multiple species, DNAMotifTokenizer demonstrates comparable or superior performance in these cross-species predictions. Specifically, DNAMotifTokenizer achieves average MCC at 0.4662 in yeast, 0.5509 in mouse (Table F.6).

Table 4: Performance of DNAMotifTokenizer and all BPEs, on five Benchmark datasets

Model	GUE Ave. MCC	SCREEN Ave. MCC	DART-EVAL Ave. ACC	Genomic Benchmark Ave. MCC	NT-Benchmarks Ave. MCC
BPE(DNABERT2)	0.6468 \pm 0.1242	0.8791 \pm 0.0224	0.8342 \pm 0.0328	0.6886 \pm 0.1721	0.5839 \pm 0.1016
BPE(hg38, 4096)	0.6638 \pm 0.122	0.8717 \pm 0.0294	0.8425 \pm 0.0408	0.7006 \pm 0.1565	0.5839 \pm 0.0945
BPE(hg38, 2048)	0.6684 \pm 0.1302	0.8743 \pm 0.033	0.8451 \pm 0.0531	0.7021 \pm 0.1584	0.595 \pm 0.1052
BPE(hg38, 1024)	0.673 \pm 0.127	0.8781 \pm 0.0269	0.8604 \pm 0.0471	0.7069 \pm 0.1556	0.5988 \pm 0.1121
BPE(motifs, 4096)	0.6522 \pm 0.1299	0.8694 \pm 0.0338	0.8309 \pm 0.0331	0.6844 \pm 0.1644	0.5764 \pm 0.0997
BPE(motifs, 2048)	0.6695 \pm 0.1273	0.8769 \pm 0.0231	0.8392 \pm 0.0499	0.6868 \pm 0.1617	0.5902 \pm 0.1057
BPE(motifs, 1024)	0.6684 \pm 0.1278	0.8777 \pm 0.0244	0.8494 \pm 0.0478	0.7005 \pm 0.163	0.5954 \pm 0.1143
BPE(cCREs, 4096)	0.6552 \pm 0.1268	0.8719 \pm 0.0333	0.8425 \pm 0.0451	0.699 \pm 0.1642	0.5723 \pm 0.0896
BPE(cCREs, 2048)	0.6645 \pm 0.1283	0.8767 \pm 0.0279	0.8382 \pm 0.0416	0.6993 \pm 0.1685	0.5973 \pm 0.1108
BPE(cCREs, 1024)	0.6743 \pm 0.1244	0.8793 \pm 0.0242	0.8458 \pm 0.0556	0.7039 \pm 0.1633	0.5954 \pm 0.1097
DNAMotifTokenizer (default)	0.6815 \pm 0.1236	0.885 \pm 0.0217	0.8437 \pm 0.0574	0.6976 \pm 0.1522	0.6018 \pm 0.1167
Ablation					
DNAMotifTokenizer (longest)	0.6687 \pm 0.1311	<u>0.8822</u> \pm 0.0237	0.8388 \pm 0.0567	0.6884 \pm 0.1639	0.5965 \pm 0.1072
DNAMotifTokenizer (shortest)	<u>0.6697</u> \pm 0.1238	0.8809 \pm 0.0303	0.8399 \pm 0.0617	0.6884 \pm 0.1549	<u>0.6003</u> \pm 0.1107

These results confirm the robustness and generalizability of DNAMotifTokenizer even outside human datasets.

Stability: We use four different seeds to run the tokenization algorithm and train four different models, and finetuned on the benchmark datasets, computed the mean and standard variation across each subdataset within each benchmark datasets. (Table G.1 G.2 G.3 G.4 G.5).

7.3 COMPLEXITY ANALYSIS

Time Complexity: The average token length in our vocabulary is approximately 8.3 nucleotides. For a genomic sequence of length n , the tokenizer proceeds sequentially from left to right, resulting in approximately $O(\frac{n}{8.3})$ tokenization steps. At each position, the tokenizer queries a Trie to identify motif tokens with lengths ranging from 4 up to Maxlen. If no motif is found, the tokenizer defaults to 3-mer or 1-mer tokens. The worst-case Trie lookup cost is $O(\text{Maxlen}^2)$. Considering potential shifts by 1 or 2 nucleotides at each position, the upper bound of the total time complexity is $O(\frac{n}{8.3} \cdot \text{Maxlen}^2)$. In our implementation, we set Maxlen = 12.

Space Complexity: Let V denote the vocabulary size and L the average token length. The Trie storing all motif tokens requires $O(V \cdot L)$ space, while the lookup table mapping motifs to token IDs takes at most $O(V)$. During tokenization, the output tokens occupy $O(\frac{n}{8.3})$ space. Therefore, the total space complexity is $O(\frac{n}{8.3} + V \cdot L)$. In our implementation, $V = 901$, the average token length is $L \approx 8.3$, and the number of motif tokens stored in the Trie is 827.

7.4 ABLATION STUDY

To evaluate the motif selection strategy, we conduct an ablation study. We test two deterministic variants: one that greedily selects the longest possible motif at each position, and another that selects the shortest (Figure 5d). While these greedy variants were still highly effective, outperforming all BPE models on three of five benchmarks, neither of these greedy strategies outperforms our default algorithm (Table 4). This finding is consistent with our earlier results, suggesting that simply optimizing for token length, and/or the nucleotide diversity in tokens, does not necessarily improve model performance. This underscores the complexity of genomic "grammar" and highlights the potential for developing more sophisticated motif selection strategies in future work.

8 CONCLUSION

In this work, we first introduce the SCREEN benchmark, a comprehensive dataset of well-annotated human functional genomic regulatory elements. Together with other benchmark datasets, we systematically evaluated state-of-the-art k-mer and BPE tokenizers under controlled settings, revealing a clear performance trade-off across different downstream tasks.

We investigated BPE optimization, finding that simply increasing vocabulary size can introduce information redundancy that harms model performance. Instead, we demonstrate that BPE tokenizers can be trained more efficiently on smaller, curated DNA sequences enriched with domain knowledge. Building on these insights, we introduce DNAMotifTokenizer, a novel tokenizer whose performance is SOTA. While our algorithm is suboptimal due to manual injections in tokenization, we highlight the necessity of incorporating domain knowledge for genomic representation learning.

Our future research will focus on (1) enhancing our approach by improving the flexibility of motif representations within the vocabulary, (2) developing a learnable tokenization algorithm, and (3) further exploring the downstream benefits for model interpretability. The ultimate goal is to advance the development of biologically informed tokenization and interpretation of genomic sequences.

REFERENCES

Garyk Brixi, Matthew G Durrant, Jerome Ku, Michael Poli, Greg Brockman, Daniel Chang, Gabriel A Gonzalez, Samuel H King, David B Li, Aditi T Merchant, et al. Genome modeling and design across all domains of life with evo 2. *BioRxiv*, pp. 2025–02, 2025.

Genome Reference Consortium. Grch38, 2013. URL <https://www.ncbi.nlm.nih.gov/assembly/88331>.

Jifeng Dai, Haozhi Qi, Yuwen Xiong, Yi Li, Guodong Zhang, Han Hu, and Yichen Wei. Deformable convolutional networks. In *Proceedings of the IEEE international conference on computer vision*, pp. 764–773, 2017.

Hugo Dalla-Torre, Liam Gonzalez, Javier Mendoza-Revilla, Nicolas Lopez Carranza, Adam Henryk Grzywaczewski, Francesco Oteri, Christian Dallago, Evan Trop, Bernardo P de Almeida, Hassan Sirelkhatim, et al. Nucleotide transformer: building and evaluating robust foundation models for human genomics. *Nature Methods*, 22(2):287–297, 2025.

Jacob Devlin, Ming-Wei Chang, Kenton Lee, and Kristina Toutanova. Bert: Pre-training of deep bidirectional transformers for language understanding. In *Proceedings of the 2019 conference of the North American chapter of the association for computational linguistics: human language technologies, volume 1 (long and short papers)*, pp. 4171–4186, 2019.

Katarína Grešová, Vlastimil Martinek, David Čechák, Petr Šimeček, and Panagiotis Alexiou. Genomic benchmarks: a collection of datasets for genomic sequence classification. *BMC Genomic Data*, 24(1):25, 2023.

Dan Hendrycks and Kevin Gimpel. Gaussian error linear units (gelus). *arXiv preprint arXiv:1606.08415*, 2016.

Tim Hulsen. Biovenn—an r and python package for the comparison and visualization of biological lists using area-proportional venn diagrams. *Data Science*, 4(1):51–61, 2021.

Yanrong Ji, Zhihan Zhou, Han Liu, and Ramana V Davuluri. Dnabert: pre-trained bidirectional encoder representations from transformers model for dna-language in genome. *Bioinformatics*, 37(15):2112–2120, 2021.

Christopher M Lee, Galt P Barber, Jonathan Casper, Hiram Clawson, Mark Diekhans, Jairo Navarro Gonzalez, Angie S Hinrichs, Brian T Lee, Luis R Nassar, Conner C Powell, et al. Ucsc genome browser enters 20th year. *Nucleic acids research*, 48(D1):D756–D761, 2020.

Yang Eric Li, Sebastian Preissl, Michael Miller, Nicholas D Johnson, Zihan Wang, Henry Jiao, Chenxu Zhu, Zhaoning Wang, Yang Xie, Olivier Poirion, et al. A comparative atlas of single-cell chromatin accessibility in the human brain. *Science*, 382(6667):eadf7044, 2023.

Yunhai Luo, Benjamin C Hitz, Idan Gabdank, Jason A Hilton, Meenakshi S Kagda, Bonita Lam, Zachary Myers, Paul Sud, Jennifer Jou, Khine Lin, et al. New developments on the encyclopedia of dna elements (encode) data portal. *Nucleic acids research*, 48(D1):D882–D889, 2020.

Camille Moeckel, Manvita Mareboina, Maxwell A Konnaris, Candace SY Chan, Ioannis Mouratidis, Austin Montgomery, Nikol Chantzi, Georgios A Pavlopoulos, and Ilias Georgakopoulos-Soares. A survey of k-mer methods and applications in bioinformatics. *Computational and Structural Biotechnology Journal*, 23:2289–2303, 2024.

Jill E Moore, Michael J Purcaro, Henry E Pratt, Charles B Epstein, Noam Shores, Jessika Adrian, Trupti Kawli, Carrie A Davis, Alexander Dobin, et al. Expanded encyclopaedias of dna elements in the human and mouse genomes. *Nature*, 583(7818):699–710, 2020.

Nature Methods. Embedding ai in biology. *Nature Methods*, 21:1365–1366, August 2024. doi: 10.1038/s41592-024-02391-7. URL <https://doi.org/10.1038/s41592-024-02391-7>.

Eric Nguyen, Michael Poli, Marjan Faizi, Armin Thomas, Michael Wornow, Callum Birch-Sykes, Stefano Massaroli, Aman Patel, Clayton Rabideau, Yoshua Bengio, et al. Hyenadna: Long-range genomic sequence modeling at single nucleotide resolution. *Advances in neural information processing systems*, 36:43177–43201, 2023.

Kazuhiro R Nitta, Arttu Jolma, Yimeng Yin, Ekaterina Morgunova, Teemu Kivioja, Junaid Akhtar, Korneel Hens, Jarkko Toivonen, Bart Deplancke, Eileen EM Furlong, et al. Conservation of transcription factor binding specificities across 600 million years of bilateria evolution. *elife*, 4: e04837, 2015.

Aman Patel, Arpita Singhal, Austin Wang, Anusri Pampari, Maya Kasowski, and Anshul Kundaje. Dart-eval: A comprehensive dna language model evaluation benchmark on regulatory dna. *Advances in Neural Information Processing Systems*, 37:62024–62061, 2024.

Lifeng Qiao, Peng Ye, Yuchen Ren, Weiqiang Bai, Chaoqi Liang, Xinzhu Ma, Nanqing Dong, and Wanli Ouyang. Model decides how to tokenize: Adaptive dna sequence tokenization with mxdna. *Advances in Neural Information Processing Systems*, 37:66080–66107, 2024.

Brian J Raney, Timothy R Dreszer, Galt P Barber, Hiram Clawson, Pauline A Fujita, Ting Wang, Ngan Nguyen, Benedict Paten, Ann S Zweig, Donna Karolchik, et al. Track data hubs enable visualization of user-defined genome-wide annotations on the ucsc genome browser. *Bioinformatics*, 30(7):1003–1005, 2014.

Ieva Rauluseviciute, Rafael Riudavets-Puig, Romain Blanc-Mathieu, Jaime A Castro-Mondragon, Katalin Ferenc, Vipin Kumar, Roza Berhanu Lemma, Jérémie Lucas, Jeanne Chèneby, Damir Baranasic, et al. Jaspar 2024: 20th anniversary of the open-access database of transcription factor binding profiles. *Nucleic acids research*, 52(D1):D174–D182, 2024.

Albin Sandelin, Wynand Alkema, Pär Engström, Wyeth W Wasserman, and Boris Lenhard. Jaspar: an open-access database for eukaryotic transcription factor binding profiles. *Nucleic acids research*, 32(suppl_1):D91–D94, 2004.

Rico Sennrich, Barry Haddow, and Alexandra Birch. Neural machine translation of rare words with subword units. *arXiv preprint arXiv:1508.07909*, 2015.

Noam Shazeer, Azalia Mirhoseini, Krzysztof Maziarz, Andy Davis, Quoc Le, Geoffrey Hinton, and Jeff Dean. Outrageously large neural networks: The sparsely-gated mixture-of-experts layer. *arXiv preprint arXiv:1701.06538*, 2017.

Nitish Srivastava, Geoffrey Hinton, Alex Krizhevsky, Ilya Sutskever, and Ruslan Salakhutdinov. Dropout: a simple way to prevent neural networks from overfitting. *The journal of machine learning research*, 15(1):1929–1958, 2014.

Gary D Stormo. Dna binding sites: representation and discovery. *Bioinformatics*, 16(1):16–23, 2000.

Mukund Sundararajan, Ankur Taly, and Qiqi Yan. Axiomatic attribution for deep networks. In *International conference on machine learning*, pp. 3319–3328. PMLR, 2017.

Ashish Vaswani, Noam Shazeer, Niki Parmar, Jakob Uszkoreit, Llion Jones, Aidan N Gomez, Łukasz Kaiser, and Illia Polosukhin. Attention is all you need. *Advances in neural information processing systems*, 30, 2017.

Emily S Wong, Dawei Zheng, Siew Z Tan, Neil I Bower, Victoria Garside, Gilles Vanwallegem, Federico Gaiti, Ethan Scott, Benjamin M Hogan, Kazu Kikuchi, et al. Deep conservation of the enhancer regulatory code in animals. *Science*, 370(6517):eaax8137, 2020.

Zhihan Zhou, Yanrong Ji, Weijian Li, Pratik Dutta, Ramana Davuluri, and Han Liu. Dnabert-2: Efficient foundation model and benchmark for multi-species genome. *arXiv preprint arXiv:2306.15006*, 2023.

APPENDIX

A DNAMOTIFTOKENIZER: TOKENIZATION ALGORITHM

Algorithm 1: Tokenization algorithm for DNAMotifTokenizer

Data: Sequence s with length n , Vocabulary $V = \{\text{motifs, 3-mer, 1-mer}\}$

Result: $y = [\text{tokens}]$

Function `Tokenize (i)`

```

score, best_token, candidates ← -1, None, []
for j ← 4 to 12 do
    seg ← substring of s from index i to i + j
    if seg ∈ motifs then
        Append seg to candidates;
if candidates ≠ None then
    best_token ← random element from candidates;
else
    if i + 3 > n then
        best_token ← 1-mer at s[i];
    else
        best_token ← 3-mer at s[i : i + 3];
next_pos ← i + length of best_token
best_score ← length of best_token
return best_token, best_score, next_pos;

```

Function `Main ()`

```

i, y ← 0, []
while i < n do
    best_token, best_score, next_pos ← None, -1, i
    for offset ← 0 to 2 do
        candidate_token, candidate_score, candidate_pos ← Tokenize (i + offset)
        if candidate_score > best_score then
            best_token ← candidate_token;
            best_score ← candidate_score;
            next_pos ← candidate_pos;
    i ← next_pos
    Append best_token to y;
return y;

```

B WHAT MAKES A GOOD BPE TOKENIZER?

B.1 SIZE MATTERS: VOCABULARY SCALING

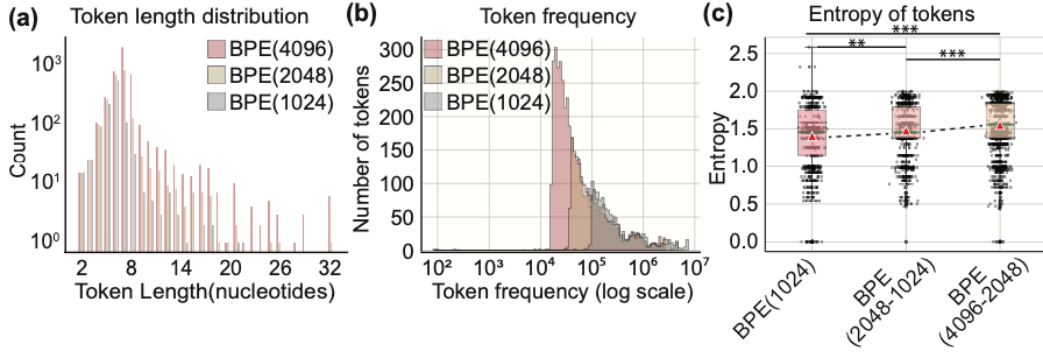


Figure B.1: Comparison across BPEs with Different Vocabulary Size. Wilcoxon test, ***, p -value < 0.001 , **, p -value < 0.01

B.2 INFORMATIVE TOKENS: ADDING DOMAIN KNOWLEDGE

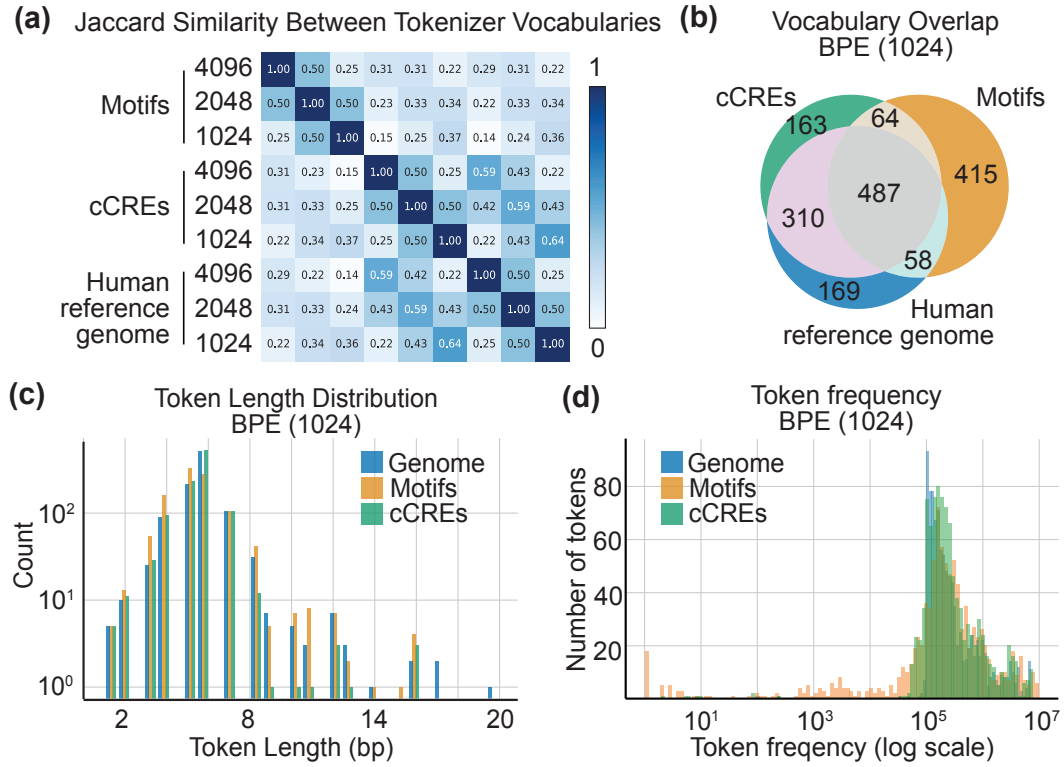


Figure B.2: Comparison across BPEs with Different Vocabulary Size and Domain Knowledge.

C MOTIF AND CCRE REGIONS

Table C.1: Jaspar Motif Annotation on hg38 Genome

Genome	Total Nucleotides at Motif Regions	Ratio (%)
hg38	1,848,048,414	59.84

Table C.2: cCRE Regions in hg38 Genome

Genome	Total cCRE Regions	Total Nucleotides at cCRE Regions	Ratio (%)
hg38	2,348,854	627,448,729	20.32

D BENCHMARKING OF STATE-OF-THE-ART TOKENIZERS

Table D.1: Performance comparison of models across datasets on GUE, grouped by task.

Dataset	3mer (overlap)	6mer (overlap)	6mer (non-overlap)	BPE (orig. DNABERT-2)	BPE (vocab size=4096)
prom_core_all	0.6645	0.6497	0.5842	0.5966	0.6270
prom_core_notata	0.6745	0.6783	0.6233	0.6421	0.6435
prom_core_tata	0.5640	0.4748	0.4919	0.5938	0.6417
prom_300_all	0.8730	0.8336	0.7871	0.8240	0.8304
prom_300_notata	0.9089	0.9022	0.8631	0.8926	0.9037
prom_300_tata	0.4643	0.5170	0.4372	0.5297	0.6006
reconstructed	0.8064	0.6434	0.6328	0.7217	0.7143
tf_0	0.6506	0.6537	0.6151	0.6402	0.6560
tf_1	0.7078	0.6908	0.6326	0.6611	0.6952
tf_2	0.5184	0.5357	0.4680	0.5587	0.5603
tf_3	0.4496	0.4304	0.3164	0.4349	0.4234
tf_4	0.6588	0.6993	0.5842	0.6657	0.6692
Mean	0.6617	0.6424	0.5863	0.6468	0.6638
Std	0.1487	0.1386	0.1482	0.1242	0.122

Table D.2: Performance comparison of models across datasets on Genomic Benchmarks

Dataset	3mer (overlap)	6mer (overlap)	6mer (non-overlap)	BPE (orig. DNABERT-2)	BPE (vocab size=4096)
human.enhancers.ensembl	0.7514	0.7771	0.6310	0.7182	0.7438
human.nontata_promoters	0.8116	0.8228	0.6975	0.8081	0.7937
demo_coding_vs_intergenic_seqs	0.8225	0.8340	0.7720	0.8113	0.8173
human.enhancers.cohn	0.4890	0.4824	0.4360	0.4565	0.4820
human.ensembl.regulatory	0.8240	0.8294	0.8678	0.8466	0.8413
human.ocr.ensembl	0.5005	0.5734	0.4569	0.4909	0.5254
Mean	0.6998	0.7199	0.6435	0.6886	0.7006
Std	0.1611	0.1528	0.1719	0.1721	0.1565

Table D.3: Performance comparison of models across datasets on Nucleotide transformer benchmarks

Dataset	3mer (overlap)	6mer (overlap)	6mer (non-overlap)	BPE (orig. DNABERT-2)	BPE (vocab size=4096)
H2AFZ	0.4727	0.5077	0.4758	0.4757	0.4916
H3K27ac	0.4460	0.4728	0.4080	0.4688	0.4914
H3K27me3	0.5720	0.5781	0.6077	0.5861	0.5983
H3K36me3	0.5972	0.6066	0.5814	0.6061	0.5955
H3K4me1	0.4598	0.4662	0.4629	0.4793	0.4804
H3K4me2	0.5692	0.5867	0.5665	0.5790	0.5741
H3K4me3	0.6537	0.6672	0.6486	0.6622	0.6736
H3K9ac	0.5201	0.5435	0.4985	0.5316	0.5390
H3K9me3	0.4227	0.4276	0.3741	0.4215	0.4271
H4K20me1	0.6064	0.6114	0.6068	0.6195	0.6074
splice_sites_donors	0.9776	0.9679	0.9503	0.6612	0.6557
splice_sites_acceptors	0.9721	0.9577	0.9163	0.6865	0.6297
splice_sites_all	0.9737	0.9655	0.9046	0.6507	0.5845
enhancers_types	0.5270	0.5596	0.4629	0.4636	0.4697
enhancers	0.5799	0.6123	0.4888	0.4741	0.5090
promoter_no_tata	0.7800	0.8169	0.7483	0.7450	0.7429
promoter_tata	0.8792	0.9093	0.6412	0.6629	0.7097
promoter_all	0.7909	0.7984	0.7228	0.7356	0.7299
Mean	0.6556	0.6697	0.6147	0.5839	0.5839
Std	0.1909	0.1838	0.1745	0.1016	0.0945

Table D.4: Performance comparison of models across datasets on SCREEN

Dataset	3mer (overlap)	6mer (overlap)	6mer (non-overlap)	BPE (orig. DNABERT-2)	BPE (vocab size=4096)
CA-CTCF	0.9099	0.9126	0.8880	0.8705	0.8702
pELS	0.9179	0.9182	0.9008	0.8897	0.8869
CA	0.9179	0.9196	0.8875	0.8777	0.8778
CA-H3K4me3	0.9132	0.9146	0.8850	0.8743	0.8657
CA-TF	0.9116	0.9126	0.8836	0.8357	0.8085
TF	0.9089	0.9086	0.8881	0.8747	0.8629
PLS	0.9342	0.9352	0.9240	0.9098	0.9013
dELS	0.9138	0.2440	0.9003	0.9006	0.9000
Mean	0.9159	0.8332	0.8947	0.8791	0.8717
Std	0.0081	0.2382	0.0135	0.0224	0.0294

Table D.5: Performance comparison across tasks on Dart-Eval(task1-3)

Dataset	3mer (overlap)	6mer (overlap)	6mer (non-overlap)	BPE (orig. DNABERT-2)	BPE (vocab size=4096)
task1	0.8668	0.8734	0.7976	0.8618	0.8631
task2	0.9919	0.9924	0.9599	0.8923	0.9327
GM12878	0.7914	0.8684	0.7896	0.8235	0.8227
H1ESC	0.7775	0.8758	0.7968	0.8178	0.8266
HEPG2	0.8165	0.8639	0.8225	0.8334	0.8312
IMR90	0.7612	0.8716	0.7619	0.7942	0.7982
K562	0.8534	0.8490	0.8419	0.8164	0.8232
Mean	0.8370	0.8849	0.8243	0.8342	0.8425
Std	0.0847	0.0465	0.0620	0.0328	0.0447

E WHAT MAKES A GOOD BPE TOKENIZER?

Table E.1: Performance comparison across datasets on GUE, with BPE trained on cCREs, varying in vocabulary size.

Dataset	BPE (cCREs, 4096)	BPE (cCREs, 2048)	BPE (cCREs, 1024)
prom_core_all	0.6173	0.6224	0.6102
prom_core_notata	0.6363	0.6405	0.6458
prom_core_tata	0.6040	0.7018	0.7130
prom_300_all	0.8338	0.8308	0.8459
prom_300_notata	0.9073	0.9069	0.9017
prom_300_tata	0.5921	0.6074	0.5965
reconstructed	0.6903	0.7383	0.7660
tf_0	0.6522	0.6431	0.6773
tf_1	0.6722	0.6662	0.6583
tf_2	0.5361	0.5437	0.5637
tf_3	0.4200	0.4052	0.4384
tf_4	0.7007	0.6673	0.6750
Mean	0.6552	0.6645	0.6743
Std	0.1268	0.1283	0.1244

Table E.2: Performance comparison across datasets on GUE, with BPE trained on motifs, varying in vocabulary size.

Dataset	BPE (motifs, 4096)	BPE (motifs, 2048)	BPE (motifs, 1024)
prom_core_all	0.6200	0.6236	0.6250
prom_core_notata	0.6296	0.6352	0.6338
prom_core_tata	0.5838	0.6811	0.6847
prom_300_all	0.8274	0.8255	0.8294
prom_300_notata	0.8941	0.9005	0.9014
prom_300_tata	0.5796	0.6310	0.5767
reconstructed	0.7362	0.7810	0.7694
tf_0	0.6574	0.6368	0.6385
tf_1	0.6820	0.6915	0.7056
tf_2	0.5508	0.5425	0.5336
tf_3	0.3947	0.4133	0.4309
tf_4	0.6708	0.6716	0.6913
Mean	0.6522	0.6695	0.6684
Std	0.1299	0.1273	0.1278

Table E.3: Performance comparison across datasets on GUE, with BPE trained on hg38, varying in vocabulary size.

Dataset	BPE (hg38, 4096)	BPE (hg38, 2048)	BPE (hg38, 1024)
prom_core_all	0.6270	0.6349	0.6254
prom_core_notata	0.6435	0.6503	0.6571
prom_core_tata	0.6417	0.6482	0.6842
prom_300_all	0.8304	0.8388	0.8298
prom_300_notata	0.9037	0.9039	0.9028
prom_300_tata	0.6006	0.5483	0.5799
reconstructed	0.7143	0.7867	0.7763
tf_0	0.6560	0.6655	0.6714
tf_1	0.6952	0.6759	0.6999
tf_2	0.5603	0.5392	0.5370
tf_3	0.4234	0.4353	0.4309
tf_4	0.6692	0.6940	0.6818
Mean	0.6638	0.6684	0.6730
Std	0.122	0.1302	0.127

Table E.4: Performance comparison across datasets on Nucleotide Transformer Benchmarks, with BPE trained on cCREs, varying in vocabulary size.

Dataset	BPE (cCREs, 4096)	BPE (cCREs, 2048)	BPE (cCREs, 1024)
H2AFZ	0.4809	0.4682	0.4751
H3K27ac	0.4765	0.4759	0.4657
H3K27me3	0.6047	0.6108	0.6052
H3K36me3	0.5775	0.5950	0.5950
H3K4me1	0.4889	0.4801	0.4909
H3K4me2	0.5642	0.5712	0.5917
H3K4me3	0.6524	0.6686	0.6812
H3K9ac	0.5308	0.5317	0.5447
H3K9me3	0.4192	0.4328	0.4309
H4K20me1	0.6171	0.6201	0.6282
splice_sites_donors	0.5983	0.7676	0.7837
splice_sites_acceptors	0.6461	0.7101	0.7047
splice_sites_all	0.5647	0.6909	0.6526
enhancers_types	0.4754	0.4624	0.4595
enhancers	0.4950	0.4999	0.4871
promoter_no_tata	0.7424	0.7406	0.7451
promoter_tata	0.6514	0.6932	0.6438
promoter_all	0.7161	0.7314	0.7313
Mean	0.5723	0.5973	0.5954
Std	0.0896	0.1108	0.1097

Table E.5: Performance comparison across datasets on Nucleotide Transformer Benchmarks, with BPE trained on motifs, varying in vocabulary size.

Dataset	BPE (motifs, 4096)	BPE (motifs, 2048)	BPE (motifs, 1024)
H2AFZ	0.4762	0.4797	0.4685
H3K27ac	0.4628	0.4600	0.4666
H3K27me3	0.5967	0.6054	0.5977
H3K36me3	0.5829	0.5859	0.5852
H3K4me1	0.4803	0.4898	0.4810
H3K4me2	0.5578	0.5613	0.5788
H3K4me3	0.6752	0.6734	0.6725
H3K9ac	0.5273	0.5294	0.5347
H3K9me3	0.3995	0.4153	0.4089
H4K20me1	0.6238	0.6380	0.6172
splice_sites_donors	0.6544	0.7533	0.7596
splice_sites_acceptors	0.5967	0.6624	0.7157
splice_sites_all	0.6109	0.6435	0.6757
enhancers_types	0.4682	0.4712	0.4565
enhancers	0.4974	0.5086	0.5079
promoter_no_tata	0.7427	0.7434	0.7529
promoter_tata	0.6932	0.6670	0.6969
promoter_all	0.7291	0.7365	0.7408
Mean	0.5764	0.5902	0.5954
Std	0.0997	0.1057	0.1143

Table E.6: Performance comparison across datasets on Nucleotide Transformer Benchmarks, with BPE trained on hg38, varying in vocabulary size.

Dataset	BPE (hg38, 4096)	BPE (hg38, 2048)	BPE (hg38, 1024)
H2AFZ	0.4916	0.4711	0.4810
H3K27ac	0.4914	0.4916	0.4802
H3K27me3	0.5983	0.6100	0.6074
H3K36me3	0.5955	0.6013	0.5950
H3K4me1	0.4804	0.4956	0.4899
H3K4me2	0.5741	0.5718	0.5835
H3K4me3	0.6736	0.6844	0.6927
H3K9ac	0.5390	0.5332	0.5497
H3K9me3	0.4271	0.4039	0.4073
H4K20me1	0.6074	0.6275	0.6214
splice_sites_donors	0.6557	0.7315	0.7448
splice_sites_acceptors	0.6297	0.6726	0.7071
splice_sites_all	0.5845	0.6406	0.6963
enhancers_types	0.4697	0.4914	0.4573
enhancers	0.5090	0.4962	0.4909
promoter_no_tata	0.7429	0.7509	0.7605
promoter_tata	0.7097	0.7120	0.6779
promoter_all	0.7299	0.7251	0.7350
Mean	0.5839	0.5950	0.5988
Std	0.0945	0.1052	0.1121

Table E.7: Performance comparison across datasets on Genomic Benchmarks, with BPE trained on cCREs, varying in vocabulary size.

Dataset	BPE (cCREs, 4096)	BPE (cCREs, 2048)	BPE (cCREs, 1024)
human_enhancers_ensembl	0.7386	0.7371	0.7473
human_nontata_promoters	0.8035	0.8144	0.8038
demo_coding_vs_intergenic_seqs	0.8224	0.8206	0.8208
human_enhancers_cohn	0.4716	0.4602	0.4681
human_ensembl_regulatory	0.8442	0.8474	0.8528
human_ocr_ensembl	0.5136	0.5164	0.5307
Mean	0.6990	0.6993	0.7039
Std	0.1642	0.1685	0.1633

Table E.8: Performance comparison across datasets on Genomic Benchmarks, with BPE trained on motifs, varying in vocabulary size.

Dataset	BPE (motifs, 4096)	BPE (motifs, 2048)	BPE (motifs, 1024)
human_enhancers_ensembl	0.7250	0.7325	0.7428
human_nontata_promoters	0.7795	0.7657	0.7984
demo_coding_vs_intergenic_seqs	0.8081	0.8078	0.8230
human_enhancers_cohn	0.4632	0.4568	0.4631
human_ensembl_regulatory	0.8377	0.8445	0.8458
human_ocr_ensembl	0.4927	0.5137	0.5301
Mean	0.6844	0.6868	0.7005
Std	0.1644	0.1617	0.163

Table E.9: Performance comparison across datasets on Genomic Benchmarks, with BPE trained on hg38, varying in vocabulary size.

Dataset	BPE (hg38, 4096)	BPE (hg38, 2048)	BPE (hg38, 1024)
human_enhancers_ensembl	0.7438	0.7449	0.7440
human_nontata_promoters	0.7937	0.7873	0.7997
demo_coding_vs_intergenic_seqs	0.8173	0.8290	0.8246
human_enhancers_cohn	0.4820	0.4740	0.4810
human_ensembl_regulatory	0.8413	0.8435	0.8477
human_ocr_ensembl	0.5254	0.5340	0.5445
Mean	0.7006	0.7021	0.7069
Std	0.1565	0.1584	0.1556

Table E.10: Performance comparison across datasets on Dart-Eval (task1-3), with BPE trained on cCREs, varying in vocabulary size.

Dataset	BPE (cCREs, 4096)	BPE (cCREs, 2048)	BPE (cCREs, 1024)
task1	0.8629	0.8663	0.8722
task2	0.9430	0.9270	0.9704
GM12878	0.8228	0.8165	0.8146
H1ESC	0.8262	0.8257	0.8223
HEPG2	0.8332	0.8298	0.8289
IMR90	0.7972	0.7988	0.7913
K562	0.8120	0.8034	0.8210
Mean	0.8425	0.8382	0.8458
Std	0.0451	0.0431	0.0602

Table E.11: Performance comparison across datasets on Dart-Eval (task1-3), with BPE trained on motifs, varying in vocabulary size.

Dataset	BPE (motifs, 4096)	BPE (motifs, 2048)	BPE (motifs, 1024)
task1	0.8599	0.8652	0.8675
task2	0.8971	0.9494	0.9594
GM12878	0.8192	0.8210	0.8245
H1ESC	0.8177	0.8197	0.8218
HEPG2	0.8223	0.8262	0.8356
IMR90	0.7913	0.7909	0.8118
K562	0.8088	0.8018	0.8248
Mean	0.8310	0.8392	0.8493
Std	0.0331	0.0499	0.0478

Table E.12: Performance comparison across datasets on Dart-Eval (task1-3), with BPE trained on hg38, varying in vocabulary size.

Dataset	BPE (hg38, 4096)	BPE (hg38, 2048)	BPE (hg38, 1024)
task1	0.8631	0.8656	0.8677
task2	0.9327	0.9658	0.9722
GM12878	0.8227	0.8216	0.8415
H1ESC	0.8266	0.8229	0.8380
HEPG2	0.8312	0.8331	0.8408
IMR90	0.7982	0.7977	0.8276
K562	0.8232	0.8093	0.8351
Mean	0.8425	0.8451	0.8604
Std	0.0408	0.0531	0.0471

Table E.13: Performance comparison across datasets on SCREEN, with BPE trained on cCREs, varying in vocabulary size.

Dataset	BPE (cCREs, 4096)	BPE (cCREs, 2048)	BPE (cCREs, 1024)
CA-CTCF	0.8723	0.8760	0.8785
pELS	0.8898	0.8924	0.8953
CA	0.8774	0.8817	0.8865
CA-H3K4me3	0.8669	0.8710	0.8734
CA-TF	0.7974	0.8145	0.8245
TF	0.8675	0.8738	0.8793
PLS	0.9032	0.9036	0.8962
dELS	0.9006	0.9003	0.9008
Mean	0.8719	0.8767	0.8793
Std	0.0333	0.0279	0.0242

Table E.14: Performance comparison across datasets on SCREEN, with BPE trained on motifs, varying in vocabulary size.

Dataset	BPE (motifs, 4096)	BPE (motifs, 2048)	BPE (motifs, 1024)
CA-CTCF	0.8719	0.8726	0.8770
pELS	0.8873	0.8910	0.8930
CA	0.8754	0.8814	0.8840
CA-H3K4me3	0.8620	0.8687	0.8715
CA-TF	0.7940	0.8295	0.8234
TF	0.8646	0.8707	0.8751
PLS	0.9006	0.9016	0.8962
dELS	0.8990	0.8997	0.9013
Mean	0.8694	0.8769	0.8777
Std	0.0338	0.0231j	0.0244

Table E.15: Performance comparison across datasets on SCREEN, with BPE trained on hg38, varying in vocabulary size.

Dataset	BPE (hg38, 4096)	BPE (hg38, 2048)	BPE (hg38, 1024)
CA-CTCF	0.8702	0.8752	0.8775
pELS	0.8869	0.8916	0.8927
CA	0.8778	0.8820	0.8843
CA-H3K4me3	0.8657	0.8678	0.8745
CA-TF	0.8085	0.7998	0.8173
TF	0.8629	0.8722	0.8752
PLS	0.9013	0.9052	0.9022
dELS	0.9000	0.9007	0.9011
Mean	0.8717	0.8743	0.8781
Std	0.0294	0.033	0.0269

F DNAMOTIFTOKENIZER

Table F.1: Performance comparison across datasets on GUE, with DNAMotifTokenizer, varying in motif matching.

Dataset	DNAMotifTokenizer (longest)	DNAMotifTokenizer (shortest)	DNAMotifTokenizer
prom_core_all	0.6412	0.6522	0.6488
prom_core_notata	0.6599	0.6413	0.6564
prom_core_tata	0.7230	0.7228	0.7195
prom_300_all	0.8355	0.8389	0.8538
prom_300_notata	0.9014	0.8945	0.9062
prom_300_tata	0.6147	0.5950	0.6441
reconstructed	0.7544	0.7603	0.7693
tf_0	0.6283	0.6379	0.6406
tf_1	0.6813	0.6581	0.6670
tf_2	0.4907	0.4883	0.5179
tf_3	0.4249	0.4756	0.4651
tf_4	0.6686	0.6711	0.6888
Mean	0.6687	0.6697	0.6815
Std	0.1483	0.1348	0.1367

Table F.2: Performance comparison across datasets on SCREEN, with DNAMotifTokenizer, varying in motif matching.

Dataset	DNAMotifTokenizer (longest)	DNAMotifTokenizer (shortest)	DNAMotifTokenizer
CA-CTCF	0.8781	0.8808	0.8822
pELS	0.8977	0.8972	0.8961
CA	0.8889	0.8890	0.8888
CA-H3K4me3	0.8764	0.8782	0.8795
CA-TF	0.8288	0.8105	0.8380
TF	0.8861	0.8820	0.8826
PLS	0.8982	0.9045	0.9087
dELS	0.9038	0.9048	0.9039
Mean	0.8822	0.8809	0.8850
Std	0.0245	0.0324	0.0253

Table F.3: Performance comparison across datasets on Nucleotide Transformer Benchmarks, with DNAMotifTokenizer, varying in motif matching.

Dataset	DNAMotifTokenizer (longest)	DNAMotifTokenizer (shortest)	DNAMotifTokenizer
H2AFZ	0.4873	0.4848	0.4835
H3K27ac	0.4822	0.4735	0.4892
H3K27me3	0.6043	0.6019	0.5994
H3K36me3	0.5963	0.5932	0.5915
H3K4me1	0.4834	0.4930	0.4814
H3K4me2	0.5890	0.5843	0.5775
H3K4me3	0.6757	0.6729	0.6701
H3K9ac	0.5264	0.5381	0.5434
H3K9me3	0.4177	0.4205	0.4170
H4K20me1	0.6197	0.6158	0.6324
splice_sites_donors	0.7230	0.7346	0.7855
splice_sites_acceptors	0.7172	0.7263	0.7309
splice_sites_all	0.6661	0.7079	0.7119
enhancers_types	0.4639	0.4672	0.4507
enhancers	0.5054	0.5053	0.4902
promoter_no_tata	0.7465	0.7544	0.7577
promoter_tata	0.6935	0.6788	0.6855
promoter_all	0.7396	0.7523	0.7342
Mean	0.5965	0.6003	0.6018
Std	0.1115	0.1123	0.1154

Table F.4: Performance comparison across datasets on Genomic Benchmarks, with DNAMotifTokenizer, varying in motif matching.

Dataset	DNAMotifTokenizer (longest)	DNAMotifTokenizer (shortest)	DNAMotifTokenizer
human_enhancers_ensembl	0.7364	0.7184	0.7426
human_nontata_promoters	0.7797	0.7606	0.7717
demo_coding_vs_intergenic_seqs	0.8207	0.8256	0.8248
human_enhancers_cohn	0.4366	0.4408	0.4505
human_ensembl_regulatory	0.8651	0.8622	0.8629
human_ocr_ensembl	0.4922	0.5227	0.5332
Mean	0.6884	0.6884	0.6976
Std	0.1748	0.1720	0.1581

Table F.5: Performance comparison across datasets on Dart-Eval (task1-3), with DNAMotifTokenizer, varying in motif matching.

Dataset	DNAMotifTokenizer (longest)	DNAMotifTokenizer (shortest)	DNAMotifTokenizer
task1	0.8609	0.8639	0.8647
task2	0.9525	0.9610	0.9571
GM12878	0.8098	0.8105	0.8206
H1ESC	0.8177	0.8155	0.8202
HEPG2	0.8271	0.8286	0.8292
IMR90	0.7862	0.7902	0.7926
K562	0.8172	0.8095	0.8217
Mean	0.8414	0.8414	0.8433
Std	0.0588	0.0613	0.0586

Table F.6: Performance of different models on Species Yeast and Mouse from GUE

Model	Epigenetic Marks Prediction(Yeast)	Transcription Factor Prediction(Mouse)
3mer(stride=1)	0.4399	0.4034
6mer(stride=1)	0.4301	0.4466
6mer(stride=6)	0.3711	0.3056
BPE(DNABERT-2)	0.4670	0.5509
DNAMotifTokenizer (longest)	0.4639	0.5306
DNAMotifTokenizer (shortest)	0.4609	0.5458
DNAMotifTokenizer	0.4662	0.5509

G STABILITY

Table G.1: Performance of DNAMotifTokenizer on GUE, across 4 seeds

Dataset	Seed 1	Seed 2	Seed 3	Seed 4	Mean	Std
prom_core_all	0.6488	0.6362	0.6484	0.6483	0.6454	0.0063
prom_core_notata	0.6564	0.6530	0.6496	0.6613	0.6551	0.0051
prom_core_tata	0.7195	0.7164	0.7164	0.6999	0.7131	0.0091
prom_300_all	0.8538	0.8412	0.8307	0.8351	0.8402	0.0095
prom_300_notata	0.9062	0.8967	0.9003	0.8994	0.9007	0.0040
prom_300_tata	0.6441	0.6049	0.6147	0.5625	0.6066	0.0332
reconstructed	0.7693	0.7620	0.7232	0.7474	0.7505	0.0202
tf_0	0.6406	0.6326	0.6631	0.6277	0.6410	0.0153
tf_1	0.6670	0.6985	0.7011	0.6871	0.6884	0.0152
tf_2	0.5179	0.5715	0.5037	0.5000	0.5233	0.0327
tf_3	0.4651	0.4742	0.4401	0.4431	0.4556	0.0162
tf_4	0.6888	0.7039	0.6725	0.6778	0.6858	0.0138

Table G.2: Performance of DNAMotifTokenizer on Nucleotide Transformer Benchmarks, across 4 seeds

Dataset	Seed 1	Seed 2	Seed 3	Seed 4	Mean	Std
H2AFZ	0.4835	0.5106	0.4831	0.4888	0.4915	0.0122
H3K27ac	0.4892	0.4663	0.4579	0.4850	0.4746	0.0142
H3K27me3	0.5994	0.6002	0.5970	0.6014	0.5995	0.0018
H3K36me3	0.5915	0.5777	0.5852	0.5957	0.5875	0.0074
H3K4me1	0.4814	0.4762	0.4763	0.4944	0.4821	0.0083
H3K4me2	0.5775	0.5938	0.5771	0.5816	0.5825	0.0076
H3K4me3	0.6701	0.6705	0.6612	0.6748	0.6692	0.0058
H3K9ac	0.5434	0.5437	0.5426	0.5452	0.5437	0.0011
H3K9me3	0.4170	0.4218	0.4202	0.4279	0.4217	0.0044
H4K20me1	0.6324	0.6277	0.6179	0.6183	0.6241	0.0069
splice sites donors	0.7855	0.7881	0.7994	0.7304	0.7759	0.0306
splice sites acceptors	0.7309	0.7288	0.7653	0.7350	0.7400	0.0165
splice sites all	0.7119	0.7072	0.7598	0.6592	0.7095	0.0418
enhancers types	0.4507	0.4580	0.4675	0.4642	0.4601	0.0071
enhancers	0.4902	0.4993	0.5120	0.4986	0.5000	0.0086
promoter no tata	0.7577	0.7642	0.7543	0.7598	0.7590	0.0041
promoter tata	0.6855	0.6707	0.6552	0.7086	0.6800	0.0225
promoter all	0.7342	0.7396	0.7333	0.7566	0.7409	0.0108

Table G.3: Performance of DNAMotifTokenizer on Genomic Benchmarks, across 4 seeds

Dataset	Seed 1	Seed 2	Seed 3	Seed 4	Mean	Std
demo human vs worm	0.9213	0.9223	0.9221	0.9179	0.9209	0.0020
dummy mouse enhancers ensembl	0.4408	0.4533	0.5031	0.4683	0.4664	0.0257
human enhancers ensembl	0.7426	0.7371	0.7355	0.7371	0.7381	0.0032
human nontata promoters	0.7717	0.7781	0.7552	0.7573	0.7656	0.0109
demo coding vs intergenic seqs	0.8248	0.8283	0.8244	0.8320	0.8274	0.0034
drosophila enhancers stark	0.3872	0.3899	0.3386	0.5248	0.4101	0.0787
human enhancers cohn	0.4505	0.4695	0.4579	0.4436	0.4554	0.0109
human ensembl regulatory	0.8629	0.8620	0.8624	0.8578	0.8613	0.0024
human ocr ensembl	0.5332	0.4986	0.5186	0.5069	0.5143	0.0147

Table G.4: Performance of DNAMotifTokenizer on SCREEN datasets, across 4 seeds

Dataset	Seed 1	Seed 2	Seed 3	Seed 4	Mean	Std
CA-CTCF	0.8822	0.8820	0.8782	0.8812	0.8809	0.0018
pELS	0.8961	0.8961	0.8981	0.8975	0.8970	0.0010
CA	0.8888	0.8843	0.8904	0.8900	0.8884	0.0027
CA-H3K4me3	0.8795	0.8777	0.8764	0.8755	0.8773	0.0018
CA-TF	0.8380	0.8086	0.8368	0.8106	0.8235	0.0162
TF	0.8826	0.8847	0.8828	0.8831	0.8833	0.0009
PLS	0.9087	0.9037	0.9033	0.9018	0.9044	0.0031
dELS	0.9039	0.9037	0.9062	0.9045	0.9046	0.0012

Table G.5: Performance of DNAMotifTokenizer on DART-EVAL datasets, across 4 seeds

Dataset	Seed 1	Seed 2	Seed 3	Seed 4	Mean	Std
task1	0.8647	0.8607	0.8625	0.8647	0.8632	0.0018
task2	0.9571	0.9564	0.9560	0.9476	0.9543	0.0044
GM12878	0.8206	0.8202	0.8077	0.8128	0.8153	0.0062
H1ESC	0.8202	0.8224	0.8163	0.8191	0.8195	0.0024
HEPG2	0.8292	0.8292	0.8259	0.8292	0.8284	0.0017
IMR90	0.7926	0.7934	0.7880	0.7802	0.7886	0.0058
K562	0.8217	0.8104	0.8124	0.8182	0.8157	0.0050

H METRICS

H.1 MATTHEWS CORRELATION COEFFICIENT

The Matthews Correlation Coefficient (MCC) is a metric for evaluating binary classification performance, particularly useful for imbalanced datasets. It takes into account true positives (TP), true negatives (TN), false positives (FP), and false negatives (FN):

$$\text{MCC} = \frac{TP \cdot TN - FP \cdot FN}{\sqrt{(TP + FP)(TP + FN)(TN + FP)(TN + FN)}}.$$

MCC ranges from -1 to $+1$, where $+1$ indicates perfect prediction, 0 corresponds to random guessing, and -1 indicates total disagreement between predictions and true labels. This makes MCC especially suitable for genomic classification tasks where class imbalance is common.

H.2 JACCARD INDEX

The Jaccard similarity index (also known as Intersection over Union) is a measure of similarity between two sets. Given two sets A and B , it is defined as:

$$J(A, B) = \frac{|A \cap B|}{|A \cup B|},$$

where $|A \cap B|$ is the number of elements common to both sets, and $|A \cup B|$ is the total number of elements in either set.

The Jaccard index ranges from 0 to 1, where 1 indicates identical sets and 0 indicates completely disjoint sets. This metric is widely used in genomics for comparing predicted regions with ground truth annotations, such as cCREs or TF binding sites.